Journal of Molecular Liquids 368 (2022) 120527

Contents lists available at ScienceDirect

Journal of Molecular Liquids

journal homepage: www.elsevier.com/locate/molliq

Structural study of water/alcohol mixtures adsorbed in MFI and MEL porosils

Paula Gómez-Álvarez [a], Eva G. Noya [b], Enrique Lomba [b]

[a] Laboratorio de Simulación Molecular y Química Computacional, CIQSO-Centro de Investigación en Química Sostenible and Departamento de Ciencias Integradas, Universidad de Huelva, 21007 Huelva, Spain
[b] Instituto de Química Física Rocasolano, CSIC, Serrano 119, E-28006 Madrid, Spain

ARTICLE INFO

Article history:
Received 11 May 2022
Revised 30 September 2022
Accepted 1 October 2022
Available online 28 October 2022

Keywords:
Water
Alcohols
Hydrogen bonds
Zeolites
Molecular simulation

ABSTRACT

Ethanol and other biofuels produced during biomass conversion must be separated from the fermentation broth (mainly water) before being used as a fuel. This can be addressed by adsorption-based separation using porous materials. The key objective of this study is to obtain a molecular understanding of water and alcohol adsorption in pure-silica zeolites, particularly in silicalite-1 (MFI-type zeolite) and silicalite-2 (MEL-type zeolite). Molecular simulation techniques are used for this purpose. They provide information on the configuration of the fluids, and so the microscopic network structure of the adsorbed polar molecules can be characterized by using a specific criterion of hydrogen bonding formation. We conducted Grand-Canonical Monte Carlo simulations to compute the adsorption isotherms of pure short alcohols and water and from the liquid alcohol/water binary mixtures throughout the composition range. Despite MFI and MEL being structurally very similar, we found differences in adsorption, which are related to the underlying molecular behavior. While water intrusion occurs by applying pressure due to stronger water-water than water–silicalite interactions, notable water adsorption from the mixture occurs first by hydrogen bond formation with the adsorbed alcohols and then by self-association. A higher degree of water clustering in MEL compared to MFI zeolite, promoted by its straight channels, leads to relatively lower uptakes of water in the latter zeolite (in favor of alcohol molecules).

1. Introduction

Undoubtedly, fossil fuels have become the dominant energy resource for the modern world. However, their prospective of depletion and rising prices of raw materials foster the search for sustainable alternatives. Currently, bioalcohols represent promising candidates, especially the first four aliphatic alcohols, with high octane rating. They are obtained in a fermentative process that takes place by means of microorganisms that convert carbohydrates extracted from plant matter. However, they represent a minor fraction of the fermentation broth, which mainly contains water. The efficient recovery of alcohols from aqueous media is challenging, representing indeed the most energy expensive step in fermentative fuel production. The traditional method of product recovery is distillation; however, it is energetically and economically undesirable in this case due to the low concentration of alcohols and their boiling point higher than that of water. The separation of the alcohols from aqueous solutions by adsorption onto porous materials is a promising alternative. A variety of adsorbent materials such as zeolites, active carbons and polymers have been employed to separate alcohols from water, but silicalite is the one most often used. Silicalite zeolites are of special interest because of their hydrophobic character among other properties.[1–12].

Since experiments on multicomponent mixtures are challenging, computational studies using molecular simulation techniques are not only a complementary but also necessary tool in this context. Initially, simulations were successfully applied to the study of adsorption onto porous materials of hydrocarbon or simple gases (*eg*, CO_2 and N_2)[13–16], but, as pointed out by Bai et al.[6], the study of the adsorption of mixtures with polar molecules is significantly more complex due to formation of hydrogen bonds and because to perform Grand Canonical Monte Carlo simulations (that allow to efficiently study the adsorption behaviour), the chemical potential of all the components of the mixture must be known. However, these data are often not available for liquid mixtures. In addition, Krishna and van Baten[17] studied the adsorption of alcohol aqueous solutions in pure silica MFI and showed that even though pure water is not adsorbed unless very high pressures are applied, significant amount of water is adsorbed from the alcohol

https://doi.org/10.1016/j.molliq.2022.120527
0167-7322/

aqueous solutions due to the formation of hydrogen bonds of water with alcohol adsorbed molecules. As a consequence, it is not possible to make predictions on the adsorption from the mixture based on the behaviour of the pure components, and this also holds for many other hydrophobic porous materials[18,19].

In spite of these difficulties, much progress has been made during the last decade, when several groups tackled the problem of the adsorption of alcohol aqueous solutions using a variety of simulation methods. Xiong et al.[1] developed a method to estimate the chemical potentials of the force-fields at the appropriate thermodynamic conditions to be used in GCMC simulations using the expanded ensemble method, but they could only access low alcohol concentrations. Bai et al.[6,7] used Gibbs-Ensemble Monte Carlo simulations in the NpT ensemble using three simulations boxes (one for the liquid, another one for the zeolite and an intermediate gas phase box, so that calculation of the chemical potentials is not needed) and extended the study of the adsorption of the alcohol aqueous solutions (methanol and ethanol) to the whole composition range, using TIP4P[20] for water and TraPPE force-field for the alcohols and silicalite[21,22]. These authors first focused on MFI[6]. Their simulations predicted a small water uptake from the liquid mixture, especially for ethanol as solute. They argued that the geometric constrains imposed by the narrow pores of MFI somewhat impeded the intrusion of water. Thus, they concluded that the optimal zeolite for water/alcohol separation should be the one with a geometry that favours the adsorption of alcohol but disfavours the formation of hydrogen bonds with water. In a subsequent computational screening study that surveyed all the zeolites in the IZA-SC[23] database, this group concluded that FER exhibits indeed better separation performance than MFI[8,7].

In a detailed structural analysis of the adsorption of water, alcohols and their mixtures in MFI using the same force-field,[24,25] this group showed that pure water adsorbs first forming dimers in the zig-zag channels, then in the straight channels and finally they enter in the intersections forming long chains. In saturation, almost half of the water molecules are involved in two hydrogen bonds, giving an average number of hydrogen bonds per adsorbed water molecule of about 1.7. In the adsorption of pure methanol and ethanol, alcohols adsorb first as isolated monomers and, only when the load of the zeolites exceeds a given threshold, hydrogen bonds start to form. In saturation, the number of hydrogen bonds per molecule for methanol and ethanol are estimated to be about 0.9 and 0.7, respectively. Regarding the adsorption from the mixtures they concluded that water molecules are often found surrounded by two alcohol molecules, which can be partly explained because their simulations predict a low water uptake.

In a recent study[26], we made a comparative study of the adsorption of alcohol/water binary mixtures in silicalite-1 and silicalite-2 for methanol, ethanol and 1-butanol at 298 K and 323 K, the typical temperatures in sugar fermentation[27,28]. Our intention was to study the different adsorption behaviour when the zig-zag channels of MFI (which showed the higher affinity for water and alcohol adsorption[6]), were remplazed by straight channels of MEL. In this work, the alcohols and the zeolites were modelled using the TraPPE force-field[22,21], but differently from the work of Bai et al.[6], TIP4P/2005[29] was used for water. Another key difference with the work of Bai et al.[6] was that we obtained estimations of the chemical potentials required for the GCMC simulations from experimental liquid–vapor curves rather than making explicit calculations for the chosen force-field. Even though this route is not methodologically consistent, it might partially correct some of the deficiencies of the force-field to predict the phase equilibria of the mixtures[26]. We found that these differences in the simulation protocol, especially the choice of the force-field, had some impact on the results. On the one hand, the chosen water model led to significantly different results on the amount of water uptake, being significantly larger for TIP4P/2005, but had a negligible effect on the alcohol adsorption. It is possible that these differences between both water models might be reduced by using the chemical potentials calculated for the corresponding force fields instead of from experimental vapor pressures, but the crossed water-alcohol interactions might also play a significant role. Unfortunately, as most experiments only provide information about the alcohol uptake[30], it is not presently possible to know which scenario occurs in reality. On the other hand, we also found that the choice of the chemical potential seems to shift the curve of alcohol uptake as a function of the liquid alcohol concentration to slightly higher concentrations when compared to the results of Bai et al.[6] that use the chemical potentials at LVE predicted by the force-field. Our main conclusion (under these assumptions) was that the zigzag channels of MFI zeolite induce slightly higher affinity for alcohols, which leads to higher adsorption selectivities compared to MEL zeolite.

In this work, we investigate the fluid structure within the pores of the MFI and MEL zeolites, which is key to understand the separation processes from a microscopic level. For aqueous solutions of alcohols, hydrogen bonding (HB) unquestionably plays a main role. While experimental techniques such as Raman spectroscopy or IR can probe the hydrogen bonds formation indirectly, molecular simulation provides straightforward information to this end, namely coordinates of all the atoms for a set of the instantaneous configurations, i.e. the most detailed structural information at the molecular scale. HB formation can then be directly computed on the basis of specific geometric or energetic criteria. Given the significantly different water uptake in MFI depending on the water force field[26,6], this study might also help to understand the origin of such differences.

The remainder of the paper is organized as follows: In Section 2, we include descriptions of the considered frameworks and provide the used models, force fields, and other simulation details. In Section 3, we comprehensively expose and discuss the results. Finally, some concluding remarks are given in Section 4.

2. Methods

2.1. Silicalite structures

Silicalite-1 (MFI-type zeolite, all-silica ZSM-5) possesses a 3D channel structure with two channel systems: Sinusoidal 10-membered-ring (MR) channels in the *x*-direction intersecting with straight 10-MR channels in the *y*-direction. Here we adopted the ortho form of MFI zeolite with *Pnma* symmetry reported by Koningsveld et al.[31] Linear channels have an approximately circular section of dimensions $5.4\text{Å} \times 5.6\text{Å}$, whereas sinusoidal channels adopt a slightly more elliptical shape of size $5.1\text{Å} \times 5.5\text{Å}$. The unit cell parameters are $a = 20.022\text{Å}, b = 19.899\text{Å}$, and $c = 13.383\text{Å}$. Silicalite-2 (MEL-type zeolite, all-silica ZSM-11) has a similar porous network, with the difference that the two sets of intersecting channels are straight, with nearly circular cross sections of dimensions $5.3\text{Å} \times 5.4\text{Å}$[32]. The crystal structure has been obtained from the International Zeolite Association[23]. Both zeolites also differ in the way of connecting channels: While MFI exhibits only one type of intersection, in MEL there are two types, a large and a small one. A schematic representation of the surface and atomic structure of both zeolites is depicted in Fig. 1.

2.2. Force fields and simulation details

The non-bonded energy potential consists of Lennard-Jones (*LJ*) 12–6 and electrostatic interactions, which were truncated at 12Å.

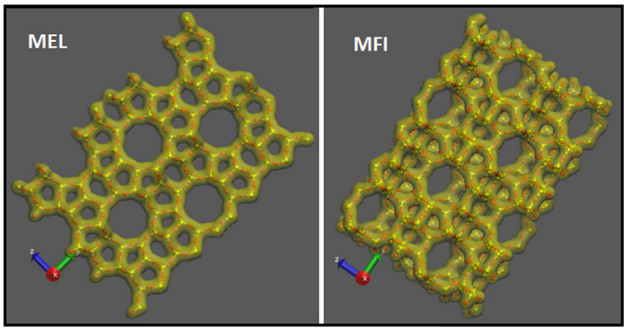

Fig. 1. Schematic representation of the surface and atomic structure of MEL (left) and MFI (right) zeolites. This view shows how the sinusoidal channels of MFI convert to straight channels in MEL.

The number of unit cells was chosen such that the minimum length of the axes of the simulation box was larger than twice the interaction cutoff distance. This corresponds to $2 \times 2 \times 2$ MFI and MEL unit cells. Periodic boundary conditions[33] were exerted in the three spatial dimensions. Long-range electrostatic interactions were evaluated using Ewald summation technique[33].

To describe the systems under study, we used models and force fields available in the literature. The zeolite structures were considered to be rigid, *i.e.*, with the framework atoms kept at their crystallographic positions. Host energies are thus neglected. The alcohols were represented by united-atom flexible models with CH_n groups taken as single-interaction sites with potential parameters from the TraPPE force field[22]. Intramolecular interactions include bond-bending and torsion potentials. The bond bending between three neighboring beads is modeled by a harmonic cosine bending potential, and changes in the torsional angle are controlled by TraPPE cosine series potential. Concerning water, we have selected the TIP4P/2005 model[29,34]. It is a rigid nonpolarizable model that considers four interacting sites placed on the three atom positions and on an additional site placed in the bisector of the angle formed by the molecule bonds. The characteristic parameters of both UA-TraPPE and TIP4P/2005 can be found in the original papers[22,29,21]. To describe *LJ* parameters and charges of the framework atoms, we used TraPPE-zeo,[21] which was originally developed to use in conjunction with the TraPPE force field for the adsorbates. Lorentz-Berthelot mixing rules were used to account for the *LJ* parameters of crossed interactions.

In order to study the adsorption from the liquid phase for the aqueous solutions of the short-chain alcohols in silicalites, we considered a binary mixture three-phase equilibrium: Equilibrium between liquid and gas (with compositions and densities determined experimentally or through an *EoS*), and equilibrium between gas and zeolite determined by means of *GCMC* simulations. The required equilibrium conditions between the liquid phase and the adsorbed phase are calculated using the fugacities corresponding to the vapor–liquid equilibrium. In this way the composition (and hence the chemical potential of each species) of the reservoir in equilibrium with the adsorbed phase are defined for the *GCMC* simulations[35,36]. The fugacities corresponding to different liquid-phase concentrations were taken from *VLE* data reported in Pemberton et al.[37] for ethanol/water mixtures and in Gmehling et al.[38] for methanol/water. The *GCMC* simulations were performed at ambient temperature using RASPA code [39,40]. In this ensemble, the chemical potential is determined from the fugacity, which is the effective thermodynamic pressure. We used Peng–Robinson equation of state[41] for fugacity/pressure conversion. We defined a *GCMC* cycle as *N* moves, including molecular swap with the reservoir, rotation, translation, and also identity change moves, which is highly recommended at high loadings. *N* denotes the number of adsorbed molecules if it is larger than 20, and 20 otherwise. Long simulations (one million *MC* cycles) were required to ensure good statistics since the strong intermolecular interactions for polar molecules complicate the sampling of all possible configurations. Complementary *GCMC* simulations were likewise conducted to examine the adsorption behavior of the pure compounds. For the case of water, adsorption occurs only at pressure much higher than the condensation pressure. In this case, we used an equation of state taken from Pršlja et al.[18] to relate the chemical potential with the pressure.

2.3. Hydrogen bonding

Configurations from simulations taken every 1000 cycles were used to calculate average hydrogen bonding properties and molecular coordination in the unary and binary systems. We compute the following properties characterizing the structure of the adsorbed fluids: The fraction of molecules in the monomer or associated state, the number of hydrogen bonds per molecule n_{HB}, and the fraction of molecules with 0 (monomers), 1, 2, 3, and 4 hydrogen bonds f_0, f_1, f_2, f_3, f_4. The number of hydrogen bonds between each pair of fluid molecules was computed by using a specific criterion to define HB formation. In the geometric definition, two molecules are considered to be associated via H-bonds if they satisfy some criteria as to their relative position and orientation[42]. Specifically, two water molecules were considered to be hydrogen bonded if *(1)* the $O \cdots O$ separation is less than 3.6Å, *(2)* the $O \cdots H$ separation is less than 2.4Å, and *(3)* the $O \cdots O - H$ angle, where H is the hydrogen atom that forms the bond, is less than 30°[43,44]. For alcohol-alcohol interactions, we considered 3.5Å and 2.6Å as threshold $O \cdots O$ and $O \cdots H$ distances, respectively [45,46]. These geometric criteria for water and alcohols are well-established [43,44,47,45,46], with threshold distance values corresponding to the positions of the first minima in the respective radial distribution functions. We have checked that the positions of the characteristic extrema remain virtually unchanged regardless of the fugacity and of the zeolite, and equal to the values for the pure bulk compounds. Hence, a geometric criterion for HB analysis of these systems, as well as the bulk geometric parameters, seems to be adequate. In Calero et al.,[48] it was already shown to account for hydrogen bonding of water in pure silica zeolites. Anyway, the geometric parameters are not too restrictive[49] and due to their close values, the same criteria are sometimes used for both alcohols and water, for the sake of simplicity. Indeed, for the cross alcohol-water interactions, we considered the same geometric parameters as those for alcohol-alcohol interactions. Overall, the error on the H-bond statistics is estimated to be less than 5%. Finally, it is worth noting that an alternative method based on energetics is also commonly used in the literature to determine the number of hydrogen bonds. However, both routes usually provide consistent results (see Ref.[50] and references therein).

3. Results

Fig. 2 shows the adsorption isotherms of pure water and alcohols, taken from our previous work,[26] together with the analysis of hydrogen bonding along the adsorption process for each compound. Note that the data is plotted as a function of fugacity, which in the case of water is not equal to the effective thermodynamic pressure. In our previous work[26], to make this conversion we used an equation of state fitted to simulation data[18] and found that water adsorption occurs at pressures of about 10^8 Pa, in close agreement to simulation results using TIP4P[51,52,6] and to experimental data measured using zeolite samples with very low defect concentrations[52]. The adsorption isotherms of the alcohols were

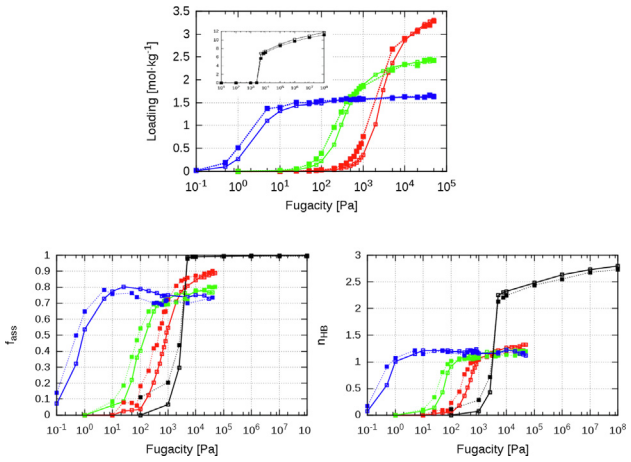

Fig. 2. Upper graph[26]: Pure adsorption isotherms (top) at 298*K* of methanol (red), ethanol (green), 1-butanol (blue) and water (black) in pure-silica MFI (dotted lines) and MEL (continuous lines) zeolites. Lower graphs: The underlying fraction of associated molecules f_{ass} (bottom left) and average number of hydrogen bonds per molecule n_{HB} (bottom right) as a function of fugacity.

compared with experimental data by Dubinin et al.[53] for MFI and with our own measurements for MEL, finding a fairly good agreement between simulations and experiments. As well, good agreement was found with simulated data from Bai et al.[6] for unary adsorption of methanol and ethanol in MFI. For a more detailed comparison, see our previous work[26]. In the bottom two panels of Fig. 2 we report, as a function of the fugacity, the fraction of associated molecules f_{ass} and the number of hydrogen bonds per molecule n_{HB}. We used the above introduced geometric criterion for HB definition to compute these properties. A clear enhancement of hydrogen bonding occurs as the pressure (and thus loading) increases.

As it is apparent from the fraction of associated molecules, HB formation gains importance with pressure and associated alcohol molecules prevail over monomers (f_{ass} above 0.5) from 1*Pa* (1-butanol), 100*Pa* (ethanol) and 1000*Pa* (methanol), approximately, which correspond to the pressures at which the adsorption isotherms increase. Although at the highest coverages association dominates, the number of monomers is not negligible at all. The fraction of associated molecules at saturation decreases with increasing molecular size of the alcohol, with values of about 0.9, 0.8 and 0.7 for methanol, ethanol and 1-butanol, respectively. Curiously, for 1-butanol, the degree of association slightly decreases at fugacities betwen 10 and 10^5 Pa. This is likely due to steric effects. The increase of loading favors association but the excessive molecular packing for high fugacities somewhat hinders hydrogen bond formation. In the case of pure water, the rapid pore filling phenomenon implies the absence of monomers. Virtually all the molecules are associated (bulk-like behavior) after the steep condensation.

The average number of hydrogen bonds per molecule n_{HB} is related to the degree of association. Overall, as the fugacity grows, so does the n_{HB} values, i.e., more complex hydrogen-bonded clusters are formed. Whereas the rapid intrusion of pure water leads directly to a dense phase within the pores, the degree of association gradually increases with coverage for the alcohols. At saturation, n_{HB} value ranges between 1 and 1.5 (chain-like structure) for the alcohols, and between 2 and 3 for water. Due to the confinement, these values lie well below those of the bulk using the same models, namely 1.89 and 3.52, respectively. These data on bulk fluids are consistent with previous works[43,46,48]. Therefore, although these polar molecules remain highly structured at complete filling in these zeolites, they form a weaker HB network compared to the bulk phase. Additionally, the curves of adsorption isotherms and of n_{HB} *vs fugacity* display similar shapes, which denotes strong correlation between these macroscopic and microscopic descriptions. This can be understood as an indication that pore filling mechanisms are mostly driven by hydrogen bonding.

Next, we compare our results on the structural analysis with available data for single-component adsorption of water and alcohols in MFI zeolite. In the case of water, the average number of hydrogen bonds per molecule n_{HB} obtained in this work for the adsorbed phase in MFI zeolite (about 2.7) is quite consistent with the percentages of molecules engaged in hydrogen bonds reported in Desbiens et al. [52], which imply a n_{HB} value of about 2.3, taking into account: *(i)* the use of different water models: TIP4P/2005[29] and TIP4P[20], respectively, *(ii)* the use of different zeolite frameworks: taken from Koningsveld et al.[31] and Olson et al.[54], respectively, and *(iii)* that the value reported by Desbiens et al. [52] corresponds to complete filling, and the steric effects of the excessive molecular packing can lead to a decrease of this property, as commented above for the unary adsorption of 1-butanol. Wang et al.[24] however reported for adsorbed water in silicalite-1 at 252 MPa a considerably lower n_{HB} value of 1.7. As in Desbiens et al. [52], they used the TIP4P model [20] for describing water. The zeolite structure was taken in this case from the IZA database[23], but we believe that the discrepancy is too large to be ascribed to the source of the zeolite framework. In our opinion, it can be due to the used software/algorithms for HB analysis. Indeed, the n_{HB} value for bulk water reported in Wang et al. [24], 2.9, is likewise lower than that estimated in previous work[55] using the same force field, of about 3.4, which is consistent with the fact that the vast majority of molecules are engaged in 4 hydrogen bonds. Atomistic water models available in the literature (three, four of five-site) generally provide the number of hydrogen bonds per molecule at least above 3. This is indicative of likely underestimation of this property in Wang et al. [24], with values for adsorbed water in MFI that are quite below those predicted by us and by Desbiens et al.[52], as just commented. In the case of the alcohols, we obtain n_{HB} values slightly above 1 for saturated phases in MFI for both methanol and ethanol, whereas Wang et al. [24] reported values of 0.9 and 0.7, respectively. The discrepancy in this case is lesser than that for water, and likely also ascribed to the methodology of hydrogen bonding analysis, which seems to somewhat underestimate this property for both adsorbed and bulk phases.

To the best of our knowledge, there is not available data for comparison in MEL zeolite. The comparison of the structural analysis obtained here for both MFI and MEL zeolites (dotted *vs* continuous lines, respectively) shows a slightly more complex HB network for the alcohols in MFI zeolite and for water in MEL zeolite during the adsorption process, if they are compared at the same pressure. Results at saturation loadings are almost the same. Since adsorption in the low-coverage regime is directly related to the affinity of the molecules with the surface of the adsorbent, we depict in Fig. 3 the average density plots of ethanol in both silicalites at low loadings – 200*Pa* –. The probability of finding a molecule in a given position of the zeolite is indicated by the color scale in the left. As it is apparent from these plots, intersections are the preferential adsorption sites in both zeolites, but also the zig-zag channels in MFI zeolite, which explains the larger uptakes of alcohol in this latter zeolite. Similar behavior was found for methanol and 1-butanol. In the case of water, an abrupt condensation transition takes place only by applying hydraulic pressure, due to hydrophobic nature and small diameter of the zeolite channels. Consequently, the average density plots of water convey little information of interest.

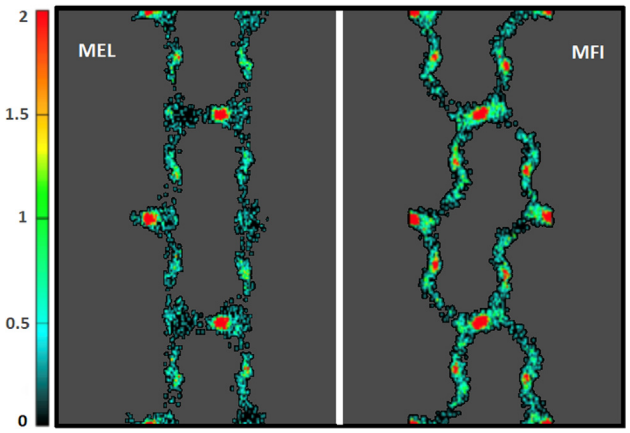

Fig. 3. Average density plots of ethanol in pure silica MEL (left) and MFI (right) zeolites at low loadings (at 200*Pa* in particular).The relation between colour and probability density occupation (from blue to red) is shown in the bar colour ramp situated on the left side of the figure. It is worth noting that similar images were included in the Graphical Abstract of our previous work[26],but just with the end of improving its visual aspect; they were not dealt and discussed in the text.

Further insight on the role played by guest-framework surface interactions is provided by two quantities plotted in Fig. 4: the average self-coordination per adsorbate molecule, and the average coordination with the oxygen atoms of the zeolites. In order to be consistent with the HB criterion introduced above, self-coordination is defined in terms of a distance of 3.5Å, and the same value is used for assessing the coordination with zeolite oxygen atoms. Since no angular criterion is being used, average coordination numbers will be larger than the average number of H-bonds per molecule – see Fig. 2–. Overall, the coordination of the guest molecules around the oxygen atoms of the framework surface decreases with increasing the molecular size, which is due to steric effects. The different trends with fugacity of these curves for alcohol and water molecules support the distinct adsorption mechanisms of these polar molecules in silicalites. Alcohols exhibit the largest coordination numbers with respect to framework oxygen atoms at the lowest coverages. This is an indication of adsorption dominated by alcohol-surface interactions (stronger than alcohol-alcohol interactions in the bulk). The larger coordination of the alcohol molecules with MFI surface is consistent with the relatively higher adsorption affinity of alcohols to the zig-zag channels of this zeolite, as commented in Fig. 3. As fugacity increases in parallel with alcohol loading, self-coordination of alcohols increases in detriment of coordination with the framework surface. In contrast, both coordination numbers increase for water with growing fugacity. The increasing coordination numbers between zeolite and water oxygen atoms with fugacity certainly show that adsorption is accomplished by applying hydraulic pressure. The opposite tendency found for alcohols reflects the energetically driven adsorption in this case, mainly ascribed to their larger molecular size. Coordination with the zeolite surface is hence mainly controlled by energetic factors for alcohols and by entropic and packing factors for water. After the sudden condensation transition of water, energetic factors due to water-water interactions obviously also play a role, as reflects the increase with fugacity of the self-coordination numbers, as well as of the average number of hydrogen bonds per water molecule (in Fig. 2).

In what follows, we address the structural analysis corresponding to the competitive alcohol/water adsorption. We report in Figs. 5 and 6 the adsorption loading at ambient temperature from methanol/water and ethanol/water binary mixtures (data replotted from our recent work)[26], respectively, as a function of the alcohol molar fraction in the liquid mixture, together with the results for the corresponding HB networks. For these zeolites and thermodynamic conditions 1-butanol is preferentially adsorbed over water throughout the composition range. Therefore, the structural analysis of the 1-butanol/water mixture adsorption is less relevant and is not presented here.

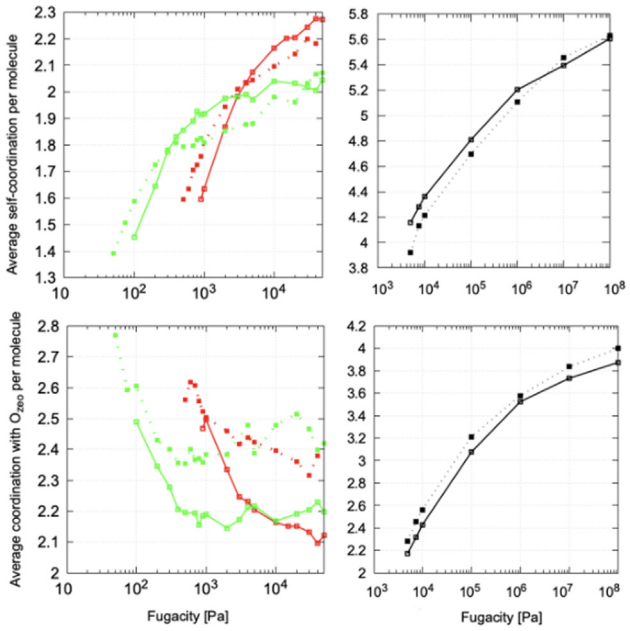

Fig. 4. Average coordination per adsorbate molecule: 3.5Å self-coordination (up) and coordination with the oxygen atoms of zeolite (down) for methanol (red), ethanol (green) and water (black) in pure-silica MFI (dotted lines) and MEL (continuous lines) zeolites as a function of fugacity. Data for 1-butanol is omitted for the sake of clarity.

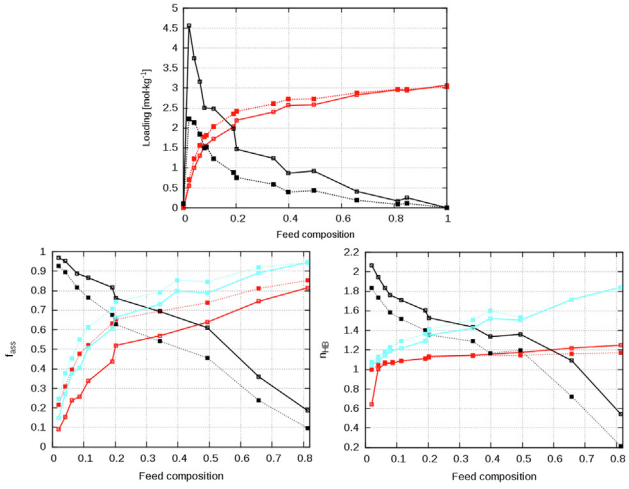

Fig. 5. Upper graph[26]: Adsorption loading of methanol (red)/ water (black) mixture in pure-silica MFI (dotted lines) and MEL (continuous lines) zeolites as a function of the feed composition (alcohol molar fraction in the liquid mixture) at ambient temperature. Lower graphs: Hydrogen bonding analysis as a function of the feed composition, namely fraction of associated molecules f_{ass} (left) and average number of hydrogen bonds per molecule n_{HB} (right). Black and red colors denote self-association for water and methanol, respectively, and blue color represents cross association referred to water (*ie*, fraction of water molecules associated with methanol molecules and average number of bonds per water molecule with methanol molecules). As commented in Section 2.2, we used experimental data of vapour-liquid equilibrium[38] from which the chemical potential at coexistence was inferred.

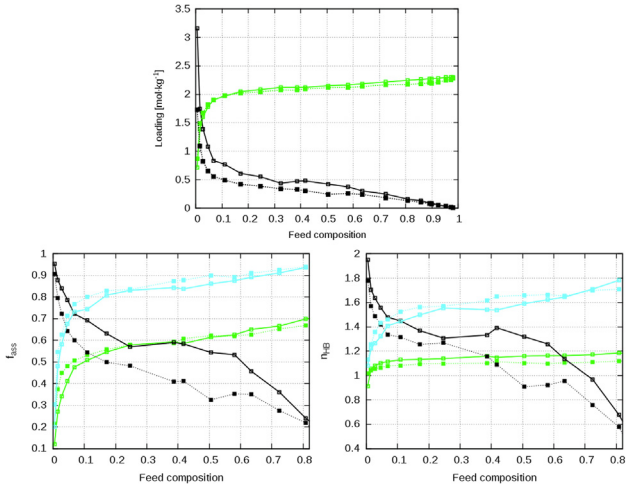

Fig. 6. Upper graph[26]: Adsorption loading of ethanol (green)/ water (black) mixture in pure-silica MFI (dotted lines) and MEL (continuous lines) zeolites as a function of the feed composition (alcohol molar fraction in the liquid mixture) at ambient temperature. Lower graphs: Hydrogen bonding analysis as a function of the feed composition, namely fraction of associated molecules f_{ass} (left) and average number of hydrogen bonds per molecule n_{HB} (right). Black and green colors denote self-association for water and ethanol, respectively, and blue color represents cross association referred to water (*ie*, fraction of water molecules associated with ethanol molecules and average number of bonds per water molecule with ethanol molecules). As commented in Section 2.2, we used experimental data of vapour-liquid equilibrium[37] from which the chemical potential at coexistence was inferred.

In our previous work[26], the amount of ethanol adsorbed as a function of alcohol concentration was compared with available experimental[56] and simulation results[6]. We found a reasonable agreement, although our data was slightly shifted to higher alcohol concentrations, probably due to the different procedure used to estimate the chemical potential for the GCMC simulations. However, our simulations predict a much higher water uptake than the simulations of Bai et al.[6]. In our previous work we showed that the choice of the water model affects critically to the water uptake, whereas adsorbed alcohol remains unaffected[26]. In particular, a small water uptake is predicted when using TIP4P[20], whereas quite large uptake is predicted by TIP4P/2005[29]. Besides, it is reasonable to think that water-alcohol cross interactions will be also relevant, but previous work has shown that the use of LB combining rules (which were used both in our work and in the simulations of Bai et al.[6]) provide a poor description of the excess properties of the bulk mixtures [57]. Note that experiments do not provide direct access to the amount of adsorbed water, thus it is not possible to know what scenario is more plausible. The difficulty of experiments to obtain information about the water uptake is discussed in the recent work of DeJaco et al.[30], and led them to resort to a combination of experimental and simulation data to get an estimate of the amount of adsorbed of water as a function of the concentration of the binary mixture. In particular, they propose to use the predicted coadsorption by simulation coupled with the bulk solute (ethanol) concentration measurements, referring this combined approach as "coadsorption method". In that regard, we do not think that these data can be used as an unambiguous proof of low water uptake in experiments, since it includes experimental bulk measurements but simulated solvent loadings, especially at low concentration. As occurs for the comparison of our results with those from Bai et al.[6], our data for ethanol adsorption (Fig. 6) agree well with this recent study [30], but our simulations predict a higher water uptake. We think that only experiments that have direct access to water uptake can solve these discrepancies between different force fields. We refer the readers to our previous work[26] for a more extensive discussion on the effects of the choice of the water model and for a more exhaustive comparison with the literature.

Moving now to the analysis of the hydrogen bond and association analysis, consistently with previous work,[17,6,19], we have found that the presence of adsorbed alcohol molecules promotes water adsorption through hydrogen bonding interactions, which in turn enhances water adsorption due to the strong water-water interactions. This is clearly apparent from the results on cross and self-association of water in the diluted alcohol concentrations. Although the presence of adsorbed water molecules is maximum from liquid mixtures of low alcohol concentrations, a non-negligible amount of water is adsorbed over a wide range of solution-phase compositions. In contrast with this, the intrusion of pure water in the silicalites can only be induced by pressure.

For the water-rich system (alcohol concentrations below 0.1), the fraction of self-associated adsorbed water molecules is above 0.80, and the average number of hydrogen bonds per molecule is about 2. As the alcohol concentration of the mixture increases, cross-association of water with alcohol molecules gains more importance, as well as self-association of the alcohol. Cross hydrogen bonding between the alcohol and water molecules prevails over self-association of the alcohol throughout the composition range, even for the alcohol-rich system. However, it is worth emphasizing in this respect that cross association is referred to water molecules. Given that for the alcohol-rich systems, a very small amount of water is adsorbed, it is not surprising that the few water adsorbed molecules are associated with high probability to alcohol molecules. It is also interesting to note that the fraction of associated molecules for the water-water interactions reaches a plateau at intermediate concentrations for ethanol but decreases steadily for methanol. On the contrary, the water-alcohol cross interactions increase with alcohol content in both cases, this raise being more pronounced for methanol. Water adsorption is initially induced in both systems by the formation of water-alcohol hydrogen bonds, but after some water is adsorbed in the zeolite, more water can be adsorbed either by forming alcohol-water or water-water hydrogen bonds. Our results indicate that the relative relevance of these two mechanisms for water adsorption as a function of composition is different in methanol and ethanol aqueous solutions. For methanol as solute, the water-water hydrogen bonds lose relevance as the alcohol content in the liquid mixture increases, whereas in the ethanol solution water-water interactions play a significant role at intermediate concentrations (alcohol molar fractions of 0.2–0.6).

The average number of hydrogen bonds per molecule n_{HB} for the adsorbed alcohols in MFI zeolite from the aqueous solution varies approximately from 1 to 1.2 from the lowest to the highest alcohol concentration, showing a plateau curve from the dilute regime. These values and curve shape are quite consistent with those reported by Bai et al. [6] However, the n_{HB} values as a function of the composition for adsorbed water obtained in this work and in Bai et al. [6] disagree. This fact likely arises from the different models considered for molecular definition: TIP4P/2005 [29] in the present work and TIP4P [20] in Bai et al. [6], which results in different water co-adsorption predictions. Besides, the choice of the water model slightly affects n_{HB} value even for pure bulk water [55]: 3.39 and 3.52 using TIP4P and TIP4P/2005 models, respectively.

Despite the similarities between MFI and MEL, and those between methanol and ethanol the adsorption mechanisms of water are clearly determined by both the zeolite type and the molecular details of the co-adsorbed alcohol. On the one hand, the curves corresponding to MFI and MEL zeolites are similarly shaped, but quantitatively non-coincident, especially for the mixture involving methanol. Adsorption of water is relatively favored in MEL zeolite, in detriment to alcohol molecules. According to

Table 1
Comparative of the adsorption behaviour from the binary mixture between the two zeolites and between the two alcohols. The ROH-zeolite affinity is estimated from the onset pressure of the unary adsorption isotherms. Each entry indicates in which of the two compared systems a given property is higher. For example the H_2O load is lower in MFI than in MEL, but the alcohol load is higher in MFI than in MEL. Consequently, the number of water-water hydrogen bonds is lower in MFI but the number of water-alcohols hydrogen bonds is higher in MFI. Note that the H_2O and ROH load are compared in molkg^{-1} and, thus, the higher ROH load observed in the methanol mixtures simply reflects its smaller size. Note that these are general conclusions, for some values of the concentration these might not hold.

	H_2O load	ROH load	n_{HB} (H_2O-H_2O)	n_{HB} (H_2O-ROH)	ROH-zeolite affinity
MFI/MEL	lower/higher	higher/lower	lower/higher	higher/lower	higher/lower
Methanol/Ethanol	higher/lower	higher/lower	higher/lower	lower/higher	lower/higher

the structural results, this larger water uptake in MEL is ascribed to a relatively more significant self-association of water, whereas cross-association of water with alcohol molecules is higher in MFI zeolite. This is likely due to the higher adsorption affinity of alcohols for MFI zeolite, and because the straight channels of MEL zeolite are geometrically more suitable for the self-association of water. On the other hand, if we compare the results for both mixtures, slightly higher degree of hydrogen bonding for confined water is observed in the mixture with methanol. The larger alkyl chain of ethanol is a handicap for HB formation. Association of water with ethanol within the pores for low feed composition is however more significant than with methanol molecules, which can be rationalized in terms of the larger adsorption uptakes of ethanol due to size effects. These results are summarized in Table 1.

Figs. 7 and 8 provide additional information concerning the microscopic behavior of adsorbed water from water-rich liquid mixtures. Fig. 7 displays the average coordination number per water molecule with respect to guest and zeolite oxygen atoms. As we have seen, coordination numbers with adsorbed ethanol are larger than that with methanol for the same low feed concentrations. The almost same coordination numbers of water with the framework oxygens in both zeolites and the larger self-coordination of water in MEL reinforce the idea that the larger water uptakes in this zeolite arises from a more favorable environment to self-association of water due to the straight channels.

In Fig. 8, we plot the HB populations of the adsorbed water as a function of the low feed composition of the liquid mixtures. We analyze the fraction of water molecules with $i = 1, 2, 3$, and 4 hydrogen bonds, f_i. Again, we can observe that the HB network of water is considerably sensitive to the type of both the zeolite and the co-adsorbed alcohol. While bulk liquid water is dominated by molecules forming 3 or 4 hydrogen bonds, the statistics relative to confinement in these systems show that the majority of adsorbed water molecules are involved in 1 or 2 hydrogen bonds. Therefore the average number of hydrogen bonds per water molecule lies in the range $1.2 \sim 2$ for the studied alcohol concentrations (Figs. 5 and 6). Confinement prevents the formation of the tetrahedral H-bonding network of water and molecules tend to build aggregates. The relatively larger values of f_1 with respect to f_2 – especially for the ethanol/water mixtures– is an indication that chain-like aggregates of water prevail over more complex networks. Also, the comparison of f_1 and f_2 values for both adsorbents confirms the higher degree of water clustering in MEL than in MFI zeolite.

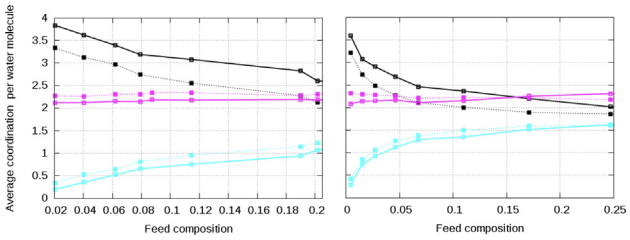

Fig. 7. Average coordination per water molecule for adsorption loadings of methanol/water (left) and ethanol/water (right) mixtures in pure-silica MFI (dotted lines) and MEL (continuous line) zeolites at low alcohol molar fractions in the liquid mixture at ambient temperature. Color code: Self-coordination (black), coordination with oxygen atoms of the alcohol (blue), and coordination with the oxygen atoms of the zeolites (pink).

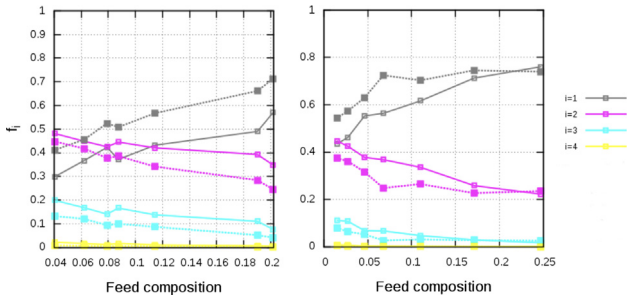

Fig. 8. Degree of self-association: Fraction of water molecules engaged in $i(= 1, 2, 3, 4)$ hydrogen bonds for adsorption loadings of methanol/water (left) and ethanol/water (right) mixtures in pure-silica MFI (dotted lines) and MEL (continuous lines) zeolites at low alcohol molar fractions in the liquid mixture at ambient temperature.

4. Conclusions

The behavior of the adsorption isotherms is closely correlated with structural changes of the adsorbed fluids. The adsorption isotherms of pure water in these pure-silica zeolites evidence an abrupt condensation transition induced by pressure. Adsorption of water from alcohols/water mixtures occurs however due to hydrogen bonding with the adsorbed alcohol molecules. These are first adsorbed due to the affinity of their alkyl chains for the hydrophobic zeolite framework, and then act as seeds for water adsorption. Subsequent self-association further promotes the adsorption of water molecules. Zig-zag channels of the MFI zeolite have a larger adsorption affinity for alcohol molecules, and are less favorable for the self-association of adsorbed water, as compared to the linear channels of MEL. These microscopic features explain the relatively more selective adsorption of short chain alcohols into MFI zeolite.

Although adsorbed water and alcohols are significantly less structured as compared to bulk fluids, the presence of hydrogen bonding still plays a crucial role. In fact, molecular association takes place already at very low coverages.

Declaration of Competing Interest

The authors declare that they have no known competing financial interests or personal relationships that could have appeared to influence the work reported in this paper.

Acknowledgements

The authors acknowledge the support from the Agencia Estatal de Investigación and Fondo Europeo de Desarrollo Regional (FEDER) under Grant No. PID2020-115722 GB-C21. Funding for open access charge: Universidad de Huelva / CBUA.

References

[1] R. Xiong, S.I. Sandler, D.G. Vlachos, Alcohol adsorption onto silicalite from aqueous solution, J. Phys. Chem. C 115 (38) (2011) 18659–18669.
[2] R. Xiong, S.I. Sandler, D.G. Vlachos, Molecular screening of alcohol and polyol adsorption onto mfi-type zeolites, Langmuir 28 (9) (2012) 4491–4499.
[3] H. Zhou, J. Mouzon, A. Farzaneh, O.N. Antzutkin, M. Grahn, J. Hedlund, Colloidal defect-free silicalite-1 single crystals: Preparation, structure characterization, adsorption, and separation properties for alcohol/water mixtures, Langmuir 31 (30) (2015) 8488–8494.
[4] A. Farzaneh, M. Zhou, E. Potapova, Z. Bacsik, L. Ohlin, A. Holmgren, J. Hedlund, M. Grahn, Adsorption of water and butanol in silicalite-1 film studied with in situ attenuated total reflectance–fourier transform infrared spectroscopy, Langmuir 31 (17) (2015) 4887–4894.
[5] K. Zhang, R.P. Lively, J.D. Noel, M.E. Dose, B.A. McCool, R.R. Chance, W.J. Koros, Adsorption of water and ethanol in mfi-type zeolites, Langmuir 28 (23) (2012) 8664–8673.
[6] P. Bai, M. Tsapatsis, J.I. Siepmann, Multicomponent adsorption of alcohols onto silicalite-1 from aqueous solution: isotherms, structural analysis, and assessment of ideal adsorbed solution theory, Langmuir 28 (44) (2012) 15566–15576.
[7] R.F. DeJaco, P. Bai, M. Tsapatsis, J.I. Siepmann, Adsorptive separation of 1-butanol from aqueous solutions using mfi-and fer-type zeolite frameworks: a monte carlo study, Langmuir 32 (8) (2016) 2093–2101.
[8] P. Bai, M.Y. Jeon, L. Ren, C. Knight, M.W. Deem, M. Tsapatsis, J.I. Siepmann, Discovery of optimal zeolites for challenging separations and chemical transformations using predictive materials modeling, Nat. Commun. 6 (2015) 5912.
[9] T. Sano, H. Yanagishita, Y. Kiyozumi, F. Mizukami, K. Haraya, Separation of ethanol/water mixture by silicalite membrane on pervaporation, J. Membr. Sci. 95 (3) (1994) 221–228.
[10] J.Z. Yang, Q.L. Liu, H.T. Wang, Analyzing adsorption and diffusion behaviors of ethanol/water through silicalite membranes by molecular simulation, J. Membr. Sci. 291 (1–2) (2007) 1–9.
[11] J.Z. Yang, Y. Chen, A.M. Zhu, Q.L. Liu, J.Y. Wu, Analyzing diffusion behaviors of methanol/water through mfi membranes by molecular simulation, J. Membr. Sci. 318 (1–2) (2008) 327–333.
[12] J. Caro, M. Bülow, J. Richter-Mendau, J. Kärger, M. Hunger, D. Freude, L.V. Rees, Nuclear magnetic resonance self-diffusion studies of methanol–water mixtures in pentasil-type zeolites, Journal of the Chemical Society, Faraday Transactions 1: Physical Chemistry in Condensed Phases 83 (6) (1987) 1843–1849.
[13] T. Düren, Y.-S. Bae, R.Q. Snurr, Using molecular simulation to characterise metal–organic frameworks for adsorption applications, Chem. Soc. Rev. 38 (5) (2009) 1237–1247.
[14] B. Smit, T.L. Maesen, Molecular simulations of zeolites: adsorption, diffusion, and shape selectivity, Chem. Rev. 108 (10) (2008) 4125–4184.
[15] Y.J. Colón, R.Q. Snurr, High-throughput computational screening of metal–organic frameworks, Chem. Soc. Rev. 43 (16) (2014) 5735–5749.
[16] J. Jiang, R. Babarao, Z. Hu, Molecular simulations for energy, environmental and pharmaceutical applications of nanoporous materials: from zeolites, metal–organic frameworks to protein crystals, Chem. Soc. Rev. 40 (7) (2011) 3599–3612.
[17] R. Krishna, J.M. van Baten, Hydrogen bonding effects in adsorption of water-alcohol mixtures in zeolites and the consequences for the characteristics if the maxwell-stefan diffusivities, Langmuir 26 (2010) 10854–10867.
[18] P. Pršlja, E. Lomba, P. Gómez-Alvarez, T. Urbič, E.G. Noya, Adsorption of water, methanol, and their mixtures in slit graphite pores, J. Chem. Phys. 150 (2) (2019) 024705.
[19] R. Krishna, J.M. van Baten, Water/alcohol mixture adsorption in hydrophobic materials: Enhanced water ingress caused by hydrogen bonding, ACS Omega 5 (2020) 28393–28402.
[20] W.L. Jorgensen, J. Chandrasekhar, J.D. Madura, R.W. Impey, M.L. Klein, Comparison of simple potential functions for simulating liquid water, J. Chem. Phys. 79 (1983) 926–935.
[21] P. Bai, M. Tsapatsis, J.I. Siepmann, Trappe-zeo: Transferable potentials for phase equilibria force field for all-silica zeolites, J. Phys. Chem. C 117 (46) (2013) 24375–24387.
[22] B. Chen, J.J. Potoff, J.I. Siepmann, Monte carlo calculations for alcohols and their mixtures with alkanes. transferable potentials for phase equilibria. 5. united-atom description of primary, secondary, and tertiary alcohols, J. Phys. Chem. B 105 (15) (2001) 3093–3104.
[23] C. Baerlocher, L.B. McCusker, Database of zeolite structures (2014). URL: http://www. iza-structure.org/databases/.
[24] C.-H. Wang, P. Bai, J.I. Siepmann, A.E. Clark, Deconstructing hydrogen-bond networks in confined nanoporous materials: implications for alcohol–water separation, J. Phys. Chem. C 118 (34) (2014) 19723–19732.
[25] T. Zhou, P. Bai, J.I. Siepmann, A.E. Clark, Deconstructing the confinement effect upon the organization and dynamics of water in hydrophobic nanoporous materials: Lessons learned from zeolites, J. Phys. Chem. C 121 (2017) 22015–22024.
[26] P. Gómez-Álvarez, E.G. Noya, E. Lomba, S. Valencia, J. Pires, Study of short-chain alcohol and alcohol–water adsorption in mel and mfi zeolites, Langmuir 34 (43) (2018) 12739–12750.
[27] Y. Lin, S. Tanaka, Ethanol fermentation from biomass resources: current state and prospects, Appl. Microbiol. Biotechnol. 69 (6) (2006) 627–642.
[28] O.J. Sanchez, C.A. Cardona, Trends in biotechnological production of fuel ethanol from different feedstocks, Bioresource technology 99 (13) (2008) 5270–5295.
[29] J.L. Abascal, C. Vega, A general purpose model for the condensed phases of water: Tip4p/2005, The Journal of chemical physics 123 (23) (2005) 234505.
[30] R. DeJaco, M.D.D. Mello, H. Nguyen, M. Jeon, R. van Zee, M. Tsapatsis, J. Siepmann, Vapor and liquid phase adsorption of alcohol and water in silicalite-1 synthesized in fluoride media, AIChE J. 66 (2020) e16868.
[31] H. Van Koningsveld, H. Van Bekkum, J. Jansen, On the location and disorder of the tetrapropylammonium (tpa) ion in zeolite zsm-5 with improved framework accuracy, Acta Crystallogr., Sect. B: Struct. Sci 43 (2) (1987) 127–132.
[32] O. Terasaki, T. Ohsuna, H. Sakuma, D. Watanabe, Y. Nakagawa, R.C. Medrud, Direct observation of "pure mel type" zeolite, Chemistry of materials 8 (2) (1996) 463–468.
[33] D. Frenkel, B. Smit, Understanding Molecular Simulation, Academic Press, 2002.
[34] C. Vega, J.L. Abascal, M. Conde, J. Aragones, What ice can teach us about water interactions: a critical comparison of the performance of different water models, Faraday discussions 141 (2009) 251–276.
[35] S. Chempath, R.Q. Snurr, J.J. Low, Molecular modeling of binary liquid-phase adsorption of aromatics in silicalite, AIChE journal 50 (2) (2004) 463–469.
[36] S. Chempath, J.F. Denayer, K.M. De Meyer, G.V. Baron, R.Q. Snurr, Adsorption of liquid-phase alkane mixtures in silicalite: simulations and experiment, Langmuir 20 (1) (2004) 150–156.
[37] R. Pemberton, C. Mash, Thermodynamic properties of aqueous non-electrolyte mixtures ii. vapour pressures and excess gibbs energies for water+ ethanol at 303.15 to 363.15 k determined by an accurate static method, J. Chem. Thermodyn. 10 (9) (1978) 867–888.
[38] J. Gmehling, U. Onken, D. Behrens, R. Eckermann, Vapor-liquid equilibrium data collection: Aqueous-organic systems, Vol. 1, Dechema Frankfurt, Germany, 1977.
[39] D. Dubbeldam, S. Calero, D.E. Ellis, R.Q. Snurr, Raspa: molecular simulation software for adsorption and diffusion in flexible nanoporous materials, Mol. Simul. 42 (2) (2016) 81–101.
[40] D. Dubbeldam, A. Torres-Knoop, K.S. Walton, On the inner workings of monte carlo codes, Mol. Simul. 39 (14–15) (2013) 1253–1292.
[41] D.B. Robinson, D.-Y. Peng, S.Y. Chung, The development of the peng-robinson equation and its application to phase equilibrium in a system containing methanol, Fluid Phase Equilib. 24 (1–2) (1985) 25–41.
[42] A. Luzar, D. Chandler, Structure and hydrogen bond dynamics of water–dimethyl sulfoxide mixtures by computer simulations, J. Chem. Phys. 98 (10) (1993) 8160–8173.
[43] J. Marti, J. Padro, E. Guardia, Molecular dynamics simulation of liquid water along the coexistence curve: Hydrogen bonds and vibrational spectra, J. Chem. Phys. 105 (2) (1996) 639–649.
[44] J. Martí, Analysis of the hydrogen bonding and vibrational spectra of supercritical model water by molecular dynamics simulations, J. Chem. Phys. 110 (14) (1999) 6876–6886.
[45] L. Saiz, J. Padro, E. Guardia, Structure and dynamics of liquid ethanol, J. Phys. Chem. B 101 (1) (1997) 78–86.
[46] M. Chalaris, J. Samios, Hydrogen bonding in supercritical methanol. a molecular dynamics investigation, J. Phys. Chem. B 103 (7) (1999) 1161–1166.
[47] J. Padró, L. Saiz, E. Guardia, Hydrogen bonding in liquid alcohols: a computer simulation study, J. Mol. Struct. 416 (1–3) (1997) 243–248.
[48] S. Calero, P. Gómez-Álvarez, Effect of the confinement and presence of cations on hydrogen bonding of water in lta-type zeolite, J. Phys. Chem. C 118 (17) (2014) 9056–9065.
[49] R. Kumar, J.R. Schmidt, J.R. Skinner, Hydrogen bonding definitions and dynamics in liquid water, J. Chem. Phys. 126 (2007) 204107.
[50] D. Swiatla-Wojcik, Evaluation of the criteria of hydrogen bonding in highly associated liquids, Chem. Phys. 342 (2007) 260–266.
[51] J.P.M. Trzpit, M. Soulard, N. Desbiens, F. Cailliez, A. Boutin, I. Demachy, A.H. Fuchs, The effect of local defects on water adsorption in silicalite-1 zeolite: A joint experimental and molecular simulation study, Langmuir 23 (2007) 10131–10139.
[52] N. Desbiens, A. Boutin, I. Demachy, Water Condensation in Hydrophobic Silicalite-1 Zeolite: A Molecular Simulation Study, J. Phys. Chem. B 109 (2005) 24071–24076.

[53] M.M. Dubinin, G.U. Rakhmatkariev, A. Isirikyan, Differential heats of adsorption and adsorption isotherms of alcohols on silicalite, Russ. Chem. Bull. 38 (1989) 1950–1953.
[54] D.H. Olson, G. Kokotailo, S.L. Lawton, W.M. Meier, J. Phys. Chem. 85 (1981) 2238–2243.
[55] S. Calero, P. Gómez-Álvarez, J. Phys. Chem. C 118 (2014) 9056–9065.
[56] B. Cekova, D. Kovec, E. Kolcakovska, D. Stojanova, Zeolites as alcohol adsorbents from aqueous solutions, Acta Period. Technol. 37 (2006) 83–87.
[57] D. González-Salgado, K. Zemánková, E.G. Noya, E. Lomba, Temperature of maximum density and excess thermodynamic properties of aqueous mixtures of methanol, J. Chem. Phys. 144 (2016) 184505.